MedCrave
Step into the World of Research
Journal of Applied Biotechnology & Bioengineering

Research Article

Open Access
CrossMark

Feasibility test of quantitative assessment of breast density based on dielectric impedance spectroscopy

Abstract

Breast density is a well-recognized important breast cancer risk factor. However, accurately assessing breast density is difficult. Although the mammographic density is the most popular method to assess breast density in current clinical practice, it is not accurate and reliable due to the overlap of breast tissues and inter-reader variability. In order to more accurately assess breast density, we proposed a new non-invasive assessment technology based on the measurement of dielectric impedance spectrums of the breast regions. The objective of this study is to test the feasibility of this new technology through a unique phantom study. The phantom design is based on mixing two types of agar saline materials with two different levels of electrical conductivity corresponding to fat and fibro-glandular tissue conductivities. In the phantom design considerations, we assembled four breast phantoms to mimic four breast density categories defined by the Breast Imaging Reporting and Data System. The testing results showed that as the increase of the simulated "fibro-glandular" tissues inside the phantom, the measured electrical impedance values monotonically decreased. The testing results were consistent and reproducible at different positions between detection probes and breast phantom surface when considering and calibrating the systematic errors. Thus, this study demonstrated the feasibility of developing and applying a new dielectric impedance measurement technology and device to assess breast density, which is low-cost, non-invasive, non-hazard and easy-to-use. If successful in future tests, this new method has potential to assist better assessing breast cancer risk for developing an optimal personalized breast cancer screening paradigm.

Keywords: breast density assessment, breast density classifications, breast cancer risk factor, breast phantom using conductive materials

Volume 2 Issue 6 - 2017

Zarafshani A,[1] Dhurjaty S,[2] Wang Y,[1] Tang S,[1] Xiang L,[1] Zheng B[1]
[1]University of Oklahoma, USA
[2]Dhurjaty Electronics Consulting LLC, USA

Correspondence: Ali Zarafshani, PhD., 101 David L Boren Blvd. Suite 1001, School of Electrical and Computer Engineering, University of Oklahoma, Norman, OK 73019, USA, Tel 405-325-3597, Email A.Zarafshani@ou.edu

Received: January 19, 2017 | **Published:** April 04, 2017

Abbreviations: BIRADS, breast imaging reporting and data system; EIT, electrical impedance tomography; EIS, electrical impedance spectroscopy

Introduction

Due to the low efficacy and controversy of the current uniform and population-based breast cancer screening using mammography,[1] developing and establishing more effective personalized breast cancer screening paradigm has been attracting extensive research interesting in the last several years.[2] The research goal aims to increase cancer detection yield (i.e., a significant increase from <0.5% in current population-based mammography screening) and/or reduce false-positive recalls, which harms many women who routinely participate in breast cancer screening. The prerequisite for the success of establishing a new optimal personalized breast cancer screening paradigm is to identify effective breast cancer risk factors that have the high discriminatory power to stratify the women into different categories or groups with different risk levels of developing or harboring breast cancers.[3] For this purpose, a large number of breast cancer risk factors have been identified and investigated in the breast cancer screening field. In the cancer epidemiology field, a number of breast cancer risk assessment models have been identified, which rely primarily on the combination of several well-known risk factors, such as age, family history, information on special genotypes and breast density.[4–6] With the exception of age and carrying specific gene mutations that only apply to a very small fraction of the population, many studies have shown that the breast density is the strongest breast cancer risk indicator.[7,8] Two well-recognized approaches to assess the breast density using mammograms were initially proposed and tested by Wolfe[9] and Pike et al.[10]

Since then, studies have investigated the correlation between mammographic tissue density and breast cancer risk. A number of studies have shown that the risk of developing breast cancer is increased between 4 to 6 times in a linear effect by growths in the dense breast tissue compared with lower mammographic breast density in the same age women.[11,12] In addition, mammographic tissue density was also shown to be associated with a number of genetic risk factors (i.e., BRCA1 and/or BRCA2 gene mutations[13]) and family history of breast cancer.[14] As a result, it is widely believed that mammographic density is an easily assessable, important and likely heritable cancer risk factor.[15] However, subjectively rating mammographic density using the Breast Imaging Reporting and Data System (BIRADS) guideline, which divides mammographic density in four categories,[16] is difficult and generates considerable inter- and intra-observer variability.[17] Thus, a number of research groups have developed computer-aided schemes to classify mammographic tissue density or patterns.[18,19] Different image features and machine learning based classifiers have been investigated and compared. Studies have reported higher correlation in assessing mammographic density between averaged visual and automated assessments (e.g., r=0.87[20]). However, mammograms are based on two-dimensional projection images. Both adipose (fat) and fibro-glandular (stroma) tissues overlap along the pass of the X-ray in one pixel. The computed pixel values are affected by a number of factors that are difficult to

be accurately controlled and/or predetermined, which include the difference of X-ray exposure and breast compression. Thus, without accurately estimating and compensating the partial volume effect, it is very difficult and unreliable to quantitatively assess the breast density.[21]

In order to overcome such difficulties, alternative approaches have also been investigated recently. Among them, studies have reported that malignant breast tissues might have 20 to 40 fold higher conductivity and capacitance than the negative breast tissues[22] and the dielectric impedance level also varies with the varying frequencies of the applied electrical field and change of the electrical properties of the breast tissue.[23] Besides *in vivo* and *in vitro* studies based on resected human tissues, a number of non-invasive electrical impedance tomography (EIT) and spectroscopy (EIS) have been developed and investigated to detect suspicious breast lesions based on the electrical impedance maps.[24–28] In order to provide a more effective tool to more accurately and conveniently assess and quantify breast density, we propose a new technology based on the non-invasive measurement of dielectric impedance signal or spectrum of the breast. The objective of this study is to conduct a special phantom study to preliminarily investigate the relationship or a variation trend between the simulated breast density levels and the measured dielectric impedance values. The details of the study concept, experimental procedures and the results are presented in the following sections of this article.

Materials and methods

Basic concept of the study

Since the dielectric impedance properties of sample tissue depend to their attractive resistivity and capacitance behavior. These behaviors are generated the magnitude and phase differences of the sample tissue. The typical dielectric impedance values of the human tissue samples at the normal conditions are different, such as blood, muscle and fat have around 150, 530 and 2060 to 2720Ωcm, respectively.[29] Thus, the electrical property of the resistance and capacitance combinations of the sample tissue within the selective permittivity is uniquely associated with the physiological properties of the living cells. The change of electrical impedance level in the specific tissues could be a useful indicator to detect or predict the abnormalities or diseases.[29] In this study, we applied a dielectric impedance signal measurement method to produce dielectric spectroscopy of different breast locations to assess and categorize breast density. The concept of the applying dielectric impedance methods is based on the similar Electrical Impedance Spectroscopy (EIS) at a multi-frequency scanning to measure the unique electrical characteristics of the human tissues. We present a desired schematic to determine the dielectric impedance spectrums based on enhanced four-electrode method. The topology utilized five electrodes to obtain two dielectric impedance measurement combinations in each injection channel, as shown in Figure 1. The transfer impedance measurement is based on two fixed electrodes that are driven by 180°C out of phase current to the target volume and other two electrodes between the current injection points, which measure the common mode voltage difference signal of the target volume.[30] For this purpose, we used a dielectric impedance analysis of two sample regions as a target volume with contact-electrodes and grain-boundaries impedances. Thus, we are able to calculate the value of the electrical impedance of the regions in regard to these impedance effects as follows:

$$Z_{Out1} = Z_{e1-contact} + Z_{e5-contact} + Z_{e2-contact} + Z_{e3-contact} + Z_{sample} + Z_{regoin1} + Z_{grain-boundary1} + Z_{grain-boundary3} + Z_{grain-boundary4} \quad (1)$$

$$Z_{Out2} = Z_{e1-contact} + Z_{e5-contact} + Z_{e3-contact} + Z_{e4-contact} + Z_{sample} + Z_{regoin2} + Z_{grain-boundary1} + Z_{grain-boundary2} + Z_{grain-boundary4} \quad (2)$$

Where the contact-impedance of the source and sink electrodes, grain-boundaries, region and sample impedances are mentioned by $Z_{electrode}$, $Z_{grain-boundary}$, Z_{sample} , Z_{region} . The corresponding circuit of the impedance spectrum involvement is demonstrated by two passive RC components in parallel. Thus, we are able to measure the dielectric impedance of different regions of the breast in order to obtain an average breast density. Applying dielectric impedance measurement of different locations of the biological tissues can provide the unique information about the electrical characteristics of the whole region. Comparison of the criteria shows a similar method to describe the electrical properties of the different breast regions. This is achieved when we are able to measure dielectric impedance spectrum of different breast locations. Based on the electrical characteristics of the different conductivities in breast tissue, we present a similar method to determine the electrical properties of the breast. The meaning of electrical properties of the region is defined by the tissue electrical properties consist of the breast. Thus, this method presents a measurement of the tissue existence in the breast by measuring the breast tissue density based on the electrical distributions. Subsequently, we suggested producing bilateral electrical properties to describe and compare dielectric impedance of the both breasts as shown in Figure 2. This is defined based on the complex impedance of the breast regions to determine the breast density level. This provides a unique contribution to determine an additional breast cancer risk feature. Essentially, the electrical impedance properties of different breast regions are similarly determined based on the mammographic density region as a clinical classification and assessment. Figure 3 shows the impedance spectrum measurement locations in order to obtain the density of the whole breast.

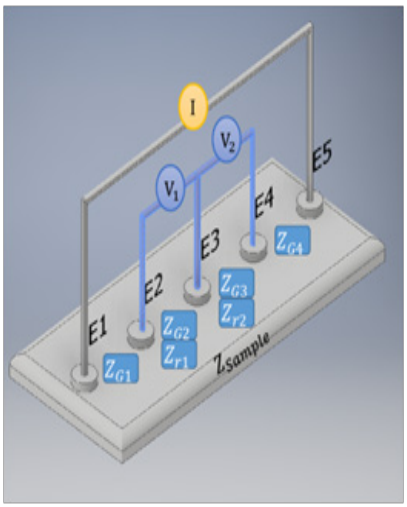

Figure 1 Enhanced Four-electrode method with an impedance analysis of two transfer impedance measurements.

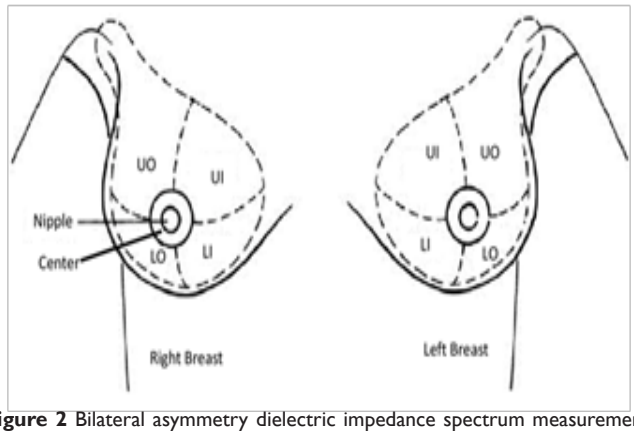

Figure 2 Bilateral asymmetry dielectric impedance spectrum measurement of left and right breasts.

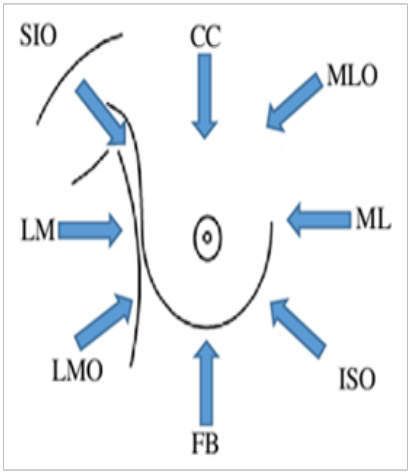

Figure 3 Suggested detection probe positions to measure dielectric impedance spectrum.

Breast phantom

The breast phantoms used in the impedance spectroscopy systems are based on physical and electrical phantoms to mimic an electrical impedance distribution of biological objects for comparison of different methods. In this study we built non-biological phantoms to simulate the biological medium for measuring dielectric impedance spectrum signals.[31] We made breast phantoms based on different tissue conductivities using different agar saline solutions. These phantoms used to simulate the different biological tissue conductivities and electrical characteristics of the breast. Briefly, since a breast mostly consists of fat and fibro-glandular tissues, the breast density could be simulated by two types of agar conductive materials of "fat tissues" as background conductivity mixed with different ratios of "fibro-glandular tissues" as a breast phantom design. These are two types of agar conductive of 0.03% and 0.185% saline solution, which correspond to have the conductivity around $\sigma_{Fat} = 0.5 mS/cm$ and $\sigma_{Stroma} = 3 mS/cm$ at 25°C.[31,32] In practice, it is difficult to create a correct conductive agar phantom. Thus, we made three specimens as illustrated in Figure 4 and measure the conductivity values. Therefore, the equivalent resistance value of 1cm^3 cube sizes of the mimicked "Fat" and "Stroma" tissues as two specimens can be obtained by Pouillet's law as follows:

$$R = \frac{L}{\sigma A} \quad (3)$$

Where,

L=Length and

A=Cross-sectional area of the specimen

The result of $R_{Fat} = 2k\Omega$, $R_{Stroma} = 333\Omega$ for "fat" and "stroma" tissues are achieved, respectively. We made four breast phantoms that consist of different percentages of saline solutions corresponding to "fat" and "fibro-glandular" tissue conductivities. The conductive agar produced by the different percentages of mixed agar and salt solution materials as illustrated in Table 1. Figure 5 shows a breast phantom cup in which two different conductive agar materials are mixed in the liquid form initially through heating. The final solid breast phantom was taken out from the cup after cooling. Therefore, four breast phantoms were built to mimic four breast density categories defined by BIRADS. In addition, two materials were not uniformly distributed inside each phantom to simulate *in vivo* conditions and producing a dynamic conductive breast phantom. The dense material may be more concentrated in one section of the phantom than other sections.

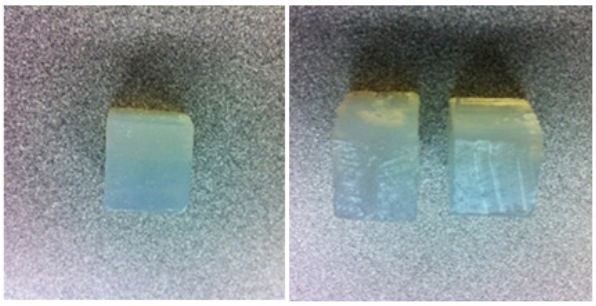

Figure 4 Illustration of the specimen with 1cm^3 cube size of "Fat" and "Stroma" tissue conductivities.

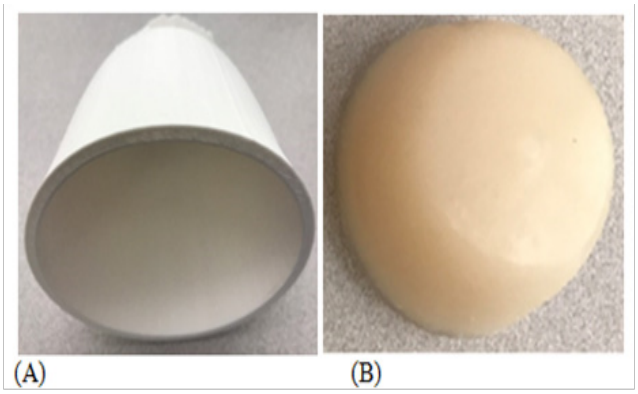

Figure 5
A. Illustration of a breast cup to make a conductive phantom and
B. A sample conductive breast phantom.

Detection of EIS signals

In the next step, we employed a SR865 DSP Lock-In Amplifier (Stanford Research Systems, Sunnyvale, CA 94089) as a signal generator and differential voltage measurements $(V_A - V_B)$. The signal generator produces the desired input Sine waves with phase

differences and operating frequency of 1mHz to 2MHz and frequency resolution of 6 digits as a reference signal passing through the custom current source using an improved Howland current source topology. The current source topology used a mirror structure to create the desired current output with 180 degree phase different.[28,30] The collecting electrical impedance signals are measured across the breast phantoms at different locations. The measured output voltages are connected to a DSP with demodulator module placed in the Lock-in Amplifier to obtain electrical impedance spectrums. This topology is capable of measuring the single-ended and differential modes with the sensitivity of 1nV to 1V (input voltage). The Sine wave based electrical current source was injected into the phantom using the model as shown in Figure 6. This model uses an enhanced four-electrode method where two electrodes (E1 and E4) inject current, while the other two electrodes (E2 and E3) and (E3 and E4) measure the potential differences of the subject under test.

Table 1 Distribution of two agar saline solutions in four breast phantoms to simulate four BI-RADS density classifications

BI-RADS density level	"Fat tissue" (0.5mS/cm)	"Fibro glandular tissue" (3mS/cm)
$0\% \xrightarrow{1^{st}\ phantom} 25\%$	75%	25%
$25\% \xrightarrow{2^{nd}\ phantom} 50\%$	60%	40%
$50\% \xrightarrow{3^{rd}\ phantom} 75\%$	40%	60%
$75\% \xrightarrow{4^{th}\ phantom} 100\%$	25%	75%

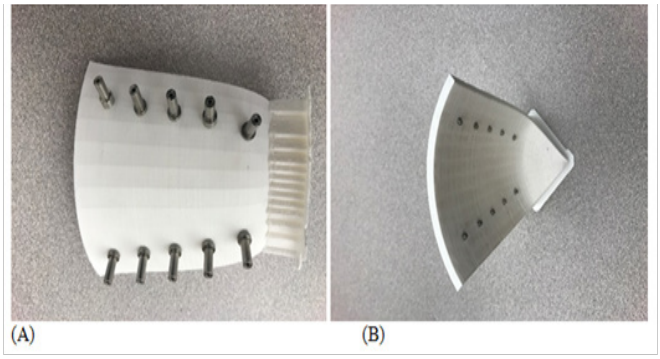

Figure 6 Illustration of the breast density transfer impedance measurement electrode plate.

The injected current source with the desired sine wave is generated by the signal generator placed in the Lock-in Amplifier. This is capable of delivering to a custom mirror structure of the improved Howland current source to obtain a nearly-constant currents regard of the voltage, which is being fed to it.[28,30] Since there is a limit on current excitation system regarding to stray and parasitic capacitances, a calibration method is performed before and during data acquisition. The differential potentials $(V_A - V_B)$ are measured on the measurement electrodes with a fixed region and grain-boundary. Therefore, two dielectric impedance spectrums are measured for each current injection. These results then used to compare with the reference signal produced by the signal generator at each frequency point. Thus, we obtain the measurement signal as follows:

$$V_{PSD} = V_{Sig} \sin\left(\omega_r t + \theta_{sig}\right) sin\left(w_L t + \theta_{ref}\right) \quad (4)$$

$$X = V_{sig} \cos(\theta) \text{ and } Y = V_{sig} \sin(\theta) \quad (5)$$

Where w_r and w_L are defined as the angular frequency of reference and output signals. Thus, we obtain:

$$V_{Sig} = R \text{ and } \theta = tan^{-1}\left(\frac{Y}{X}\right) \quad (6)$$

Therefore, an enhanced four-electrode method is used to measure two electrical impedance values in each injection channel. In each phantom, we also divided breast phantom into eight sections (as shown in Figure 3) and then repeated the experiment by placing four sets of signal detection probes to measure the output electrical impedance signals separately in each section, which correspond to 8 clock locations as shown in Figure 7.

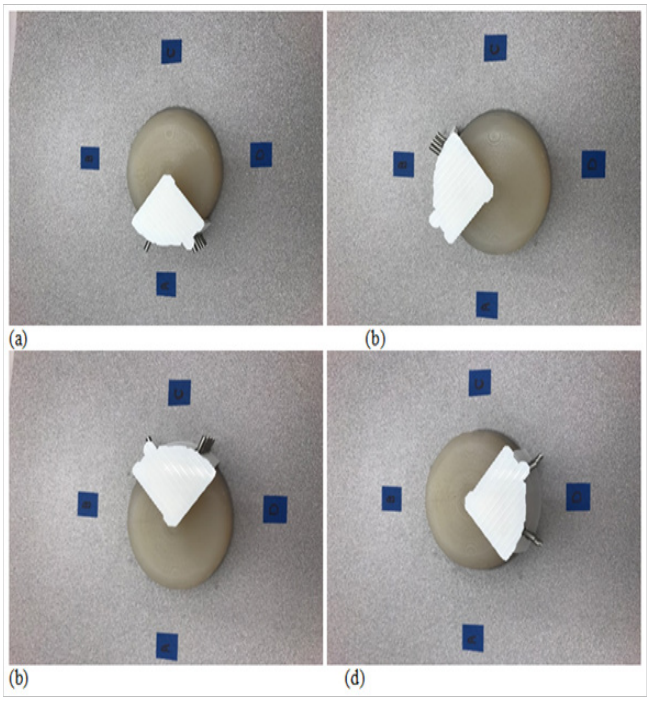

Figure 7 Illustration of repeat detection and measurement of electrical impedance signals in eight sections of a breast phantom.

Results

The detected dielectric impedance signals from multiple detection locations of four breast density phantom classifications were measured and compared. For each frequency point, we obtained the magnitude and phase difference (correspondingly In-phase, X and Quadrature, Y) of the differential voltage measurements compared to reference signal that is produced by the signal generator. Table II shows the simple data set that was evaluated for a single frequency point of 100kHz and Amplitude of 1Vpp reference signal, phase of -30° and offset of 0V. We computed dielectric impedance spectrums based on measuring output impedances at multi-frequency points. The results showed that as the increase of breast density with more percentages of the simulated "fibro-glandular" tissues, the measured dielectric impedance signal magnitudes $|Z|$ monotonically decreased. Table 2 also shows the electrical impedance signals detected from eight different locations of the left breast (as demonstrated in Figure 3) of the different density phantoms. It is worth noting that the simulated dense "fibro-glandular" tissues are not uniformly distributed inside the phantom. Thus, as expected, small variations among of eight sets of measured dielectric impedance signals occur at different o'clock positions, which shows that the dielectric impedance signal detection method is sensitive to the small change of the local density distribution. This is why we developed an enhanced four-electrode method that uses two measurement combinations in each injection channel to be able to measure the average of two close density area. The results indicate that it is feasible to correlate the measured electrical impedance signals to not only the global "fibro-glandular density" of one breast, but also the regional "dense" tissues.

Table 2 Summary of the electrical impedance measurement of single frequency point (defined as a single dataset) measured from eight positions of four breast phantoms with different density levels

Left breast locations								
Phantom 1	**CC**	**MLO**	**ML**	**ISO**	**FB**	**LMO**	**LM**	**SIO**
Magnitude	0.87	0.89	0.92	1.04	1.16	1.03	0.81	1
Phase difference θ°	-30°	-34°	-33°	-46°	-27°	-34°	-28°	-23°
X(V)	0.753	0.737	0.771	0.722	1.033	0.853	0.715	0.92
Y(V)	-0.435	-0.497	-0.501	-0.748	0.526	-0.576	-0.38	-0.39
Phantom 2	**CC**	**MLO**	**ML**	**ISO**	**FB**	**LMO**	**LM**	**SIO**
Magnitude	0.4	0.37	0.32	0.4	0.46	0.43	0.38	0.35
Phase difference θ°	-28°	-25°	-33°	-32°	-32°	-36°	-34°	-33°
X(V)	0.353	0.335	0.268	0.339	0.39	0.347	0.315	0.293
Y(V)	-0.187	-0.156	-0.174	-0.212	-0.243	-0.252	-0.212	-0.19
Phantom 3	**CC**	**MLO**	**ML**	**ISO**	**FB**	**LMO**	**LM**	**SIO**
Magnitude	0.28	0.28	0.23	0.27	0.28	0.31	0.26	0.27
Phase difference θ°	-29°	-29°	-26°	-29°	-29°	-32°	-35°	-30°
X(V)	0.244	0.244	0.206	0.236	0.244	0.262	0.212	0.233
Y(V)	-0.135	-0.135	-0.1	-0.13	-0.135	-0.164	-0.149	-0.135
Phantom 4	**CC**	**MLO**	**ML**	**ISO**	**FB**	**LMO**	**LM**	**SIO**
Magnitude	0.17	0.15	0.17	0.16	0.12	0.13	0.14	0.14
Phase difference θ°	-31°	-26°	-30°	-28°	-34°	-29°	-29°	-27°
X(V)	0.145	0.134	0.147	0.141	0.099	0.113	0.122	0.124
Y(V)	-0.087	-0.065	-0.085	-0.075	-0.067	-0.063	-0.067	-0.063

Discussion

In this study, we investigated and presented a new technology to assess and quantify breast density based on dielectric impedance property distribution. Our findings confirm that the feasibility of assessing and quantifying breast density without the use of an imaging-based modality (e.g., mammography or MRI). To the best of our knowledge, there has not been any practical test and report that uses a non-imaging based dielectric impedance spectrum measurement method to estimate and quantify breast density. This study has identified schemes to measure the electrical properties of the different breast locations to facilitate the breast density assessment with a number of unique characteristics. First, we assembled four breast phantoms with unique conductive attributes and distributions of the breast tissue to mimic the breast density based on BI-RADS categories. These phantoms were built using conductive materials to achieve the electrical properties addressing the dielectric spectroscopy of the breast. It also enables representation of the different tissue characteristics based on different saline conductive solutions. Second, the experimental result demonstrated that the measured dielectric impedance values based on characteristic of fat and glandular breast tissues are a more effective method as a clinical prototype for breast density assessment. The measured dielectric impedance signals correlated well with the percentages of the existing "fibro-glandular" tissues inside the phantoms (Table 2). Third, using the dielectric impedance measurement method cannot only non-invasive assess

Citation: Zarafshani A, Dhurjaty S, Wang Y, et al. Feasibility test of quantitative assessment of breast density based on dielectric impedance spectroscopy. *J Appl Biotechnol Bioeng.* 2017;2(6):204–210. DOI: 10.15406/jabb.2017.02.00047

global breast density, but also detect regional density difference (i.e., density focal areas), which is also extremely important for pre-screening breast cancer to detect suspicious focal dense regions.

Although this is a phantom study, experimental results and our observations are encouraging, which confirm the potential of applying this new non-invasive electrical impedance signal measurement approach in future clinical applications. This new technology offers significant advantages in assessing breast density as comparing to traditional imaging methods (i.e., mammography or breast MRI). It enables to develop a new portable dielectric impedance detection device to assess the breast density in the future, which is low-cost, safe (no-radiation), flexible, easy-to-use and without requirement of a professional image or signal interpretation as comparing to current imaging modalities for breast density measurement methods. If successful in future human tests, identification of the dielectric impedance features of breast tissues can help to generate a new clinical marker that may have higher reliability and discriminatory power to predict the risk (in particular the near-term risk) of developing breast cancer among the individual women.[33] Although recent studies have indicated that bilateral breast density asymmetry between the left and right breasts of an individual woman is potentially promising and important imaging marker to predict short-term risk for a woman developing or harbouring breast cancer,[34,35] accurate detection and quantification of bilateral mammographic density asymmetry is difficult and it is not robust enough because of both its subjective ratings of radiologists and computer-aided detection schemes, which are sensitive to the image noise variation. Moreover, the dielectric impedance measurement can be used to determine and quantify the bilateral breast density asymmetry in a simple manner and potentially more reproducible. This is a new research direction that can have a higher clinical impact to assist improve efficacy of current breast cancer screening by better stratification of women with and without risk of developing or harboring breast cancer in a short-term.

Conclusion

We presented a new non-invasive, non-imaging based method to assess breast density and demonstrated the feasibility of this new method through a unique phantom study. Despite the promising results, we recognize that this is a very preliminary phantom study. More studies are needed to improve the technology and further test the robustness of using this new dielectric impedance characteristic based application by performing human studies for non-invasively assess and quantify breast density. The results need to be compared with the breast density predicted using imaging tests such as mammograms and breast MR images and this requires further evaluation of the actual cancer screening results in the prediction of the short-term breast cancer risk.

Acknowledgements

This work is supported in part by Grants R01 CA160205 and R01 CA197150 from the National Cancer Institute, National Institutes of Health, USA. The authors would also like to acknowledge the support from the Peggy and Charles Stephenson Cancer Centre, University of Oklahoma.

Conflict of interest

The author declares no conflict of interest.

References

1. Berlin L, Hall FM. More mammography muddle: emotions, politics, science, costs and polarization. *Radiology*. 2010;255(2):311–316.
2. Gail MH. Personalized estimates of breast cancer risk in clinical practice and public health. *Stat Med*. 2011;30(10):1090–1104.
3. Schousboe JT, Kerlikowske K, Loh A, et al. Personalizing mammography by breast density and other risk factors for breast cancer: analysis of health benefits and cost-effectiveness. *Ann Intern Med*. 2011;155(1):10–20.
4. Boyd NF, Guo H, Martin LJ, et al. Mammographic density and the risk and detection of breast cancer. *N Engl J Med*. 2007;356(3):227–236.
5. Antoniou AC, Cunningham AP, Peto J, et al. The BOADICEA model of genetic susceptibility to breast and ovarian cancers: updates and extensions. *Br J Cancer*. 2008;98(8):1457–1466.
6. Ayer T, Chhatwal J, Alagoz O, et al. Informatics in radiology: comparison of logistic regression and artificial neural network models in breast cancer risk estimation. *Radiographics*. 2010;30(1):13–22.
7. Tice JA, Cummings SR, Bindman RS, et al. Using clinical factors and mammographic breast density to estimate breast cancer risk: development and validation of a new predictive model. *Ann Intern Med*. 2008;148(5):337–347.
8. Amir E, Freedman OC, Seruga B, et al. Assessing women at high risk of breast cancer: a review of risk assessment models. *J Natl Cancer Inst*. 2010;102(10):680–691.
9. Wolfe JN. Breast patterns as an index of risk for developing breast cancer. *AJR Am J Roentgenol*. 1976;126(6):1130–1137.
10. Pike MC, Krailo MD, Henderson BE, et al. 'Hormonal' risk factor, 'breast tissue age' and age-incidence of breast cancer. *Nature*. 1983;303(5920):767–770.
11. McCormack VA, Dos Santos Silva I. Breast density and parenchyma patterns as markers of breast cancer risk: a meta-analysis. *Cancer Epidemiol Biomarkers Prev*. 2006;15(6):1159–1169.
12. Boyd NF, Martin LJ, Bronskill M, et al. Breast tissue composition and susceptibility to breast cancer. *J Natl Cancer Inst*. 2010;102(16):1224–1237.
13. Vachon CM, Sellers TA, Carlson EE, et al. Strong evidence of a genetic determinant for mammographic density, a major risk factor for breast cancer. *Cancer Res*. 2007;67(17):8412–8418.
14. Martin LJ, Melnichouk O, Guo H, et al. Family history, mammographic density, and risk of breast cancer. *Cancer Epidemiol Biomarkers Prev*. 2010;19(2):456–463.
15. Tice JA, Cummings SR, Ziv E, et al. Mammographic breast density and the Gail model for breast cancer risk prediction in screening population. *Breast Cancer Res Treat*. 2005;94(2):115–122.
16. Liberman L, Menell JH. Breast imaging reporting and data system (BI-RADS). *Radiologic Clinics of North America*. 2002;40(3):409–430.
17. Berg WA, Campassi C, Langenberg P, et al. Breast imaging reporting and data system: Inter and intra-observer variability in feature analysis and final assessment. *AJR Am J Roentgenol*. 2000;174(6):1769–1777.
18. Hurst CKG, Duric N, Littrup P. A new method for quantitative analysis of mammographic density. *Med Phys*. 2007;34(11):4491–4498.
19. Wei J, Chan HP, Wu YT, et al. Association of computerized mammographic parenchymal pattern measure with breast cancer risk: a pilot case-control study. *Radiology*. 2011;260(1):42–49.

20. Chang YH, Wang XH, Hardesty LA, et al. Computerized assessment of tissue composition on digitized mammograms. *Acad Radiol*. 2002;9(8):898–905.

21. Kopans DB. Basic physics and doubts about relationship between mammographically determined tissue density and breast cancer risk. *Radiology*. 2008;246(2):348–353.

22. Chaudhary SS, Mishra RK, Swarup A, et al. Dielectric properties of normal and malignant human breast tissue at radiowave and microwave frequencies. *Indian J Biochem Biophys*. 1984;21(1):76–79.

23. Foster KR, Schwan HP. Dielectric properties of tissue and biological materials: a critical review. *Crit Rev Biomed Eng*. 1989;17(1):25–104.

24. Cherepenin V, Karpov A, Korjenevsky A, et al. A 3D electrical impedance tomography (EIT) system for breast cancer detection. *Physiol Meas*. 2001;22(1):9–18.

25. Stojadinovic A, Nissan A, Shriver CD, et al. Electrical impedance scanning as a new breast cancer risk stratification tool for young women. *J Surg Oncol*. 2008;97(2):112–120.

26. Lederman D, Zheng B, Wang X, et al. Improving breast cancer risk stratification using resonance-frequency electrical impedance spectroscopy through fusion of multiple classifiers. *Ann Biomed Eng*. 2011;39(3):931–945.

27. Zarafshani A, Huber N, Béqo N, et al. A flexible low-cost, high-precision, single interface electrical impedance tomography system for breast cancer detection using FPGA. *Journal of Physics: Conference Series*. 2010;224(1):012169.

28. Zarafshani A, Bach T, Chatwin C, et al. Current source enhancements in electrical impedance spectroscopy (EIS) to cancel unwanted capacitive effects. *Proc SPIE Medical Imaging*. 2017;10137.

29. Hope TA, Iles SE. Technology review: The use of electrical impedance scanning in the detection of breast cancer. *Breast Cancer Res*. 2004;6(2):69–74.

30. Zarafshani A. *A high-performance, multi-frequency micro-controlled Electrical Impedance Mammography (EIM) excitation and phantom validation system*. UK: University of Sussex; 2016.

31. Zarafshani A, Qureshi T, Bach T, et al. A 3D Multi-frequency response electrical mesh phantom for validation of the planar structure EIT system performance. Electro information technology (EIT), 2016 IEEE international conference; USA: IEEE; 2016. p. 600–604.

32. Jossinet J, Schmitt M. A review of parameters for the bioelectrical characterization of breast tissue. *Ann N Y Acad Sci*. 1999;873:30–41.

33. Tan M, Zheng B, Leader JK, et al. Association between changes in mammographic image features and risk for near-term breast cancer development. *IEEE Trans Med Imaging*. 2016;35(7):1719–1728.

34. Zheng B, Sumkin JH, Zuley ML, et al. Bilateral mammographic density asymmetry and breast cancer risk: a preliminary assessment. *Eur J Radiol*. 2012;81(11):3222–3228.

35. Tan M, Aghaei F, Wang Y, Zheng B. Developing a new case based computer-aided detection scheme and an adaptive cueing method to improve performance in detecting mammographic lesions. *Phys Med Biol*. 2017;62(2):358–376.

Citation: Zarafshani A, Dhurjaty S, Wang Y, et al. Feasibility test of quantitative assessment of breast density based on dielectric impedance spectroscopy. *J Appl Biotechnol Bioeng*. 2017;2(6):204–210. DOI: 10.15406/jabb.2017.02.00047